Erschienen in: Progress in Photovoltaics : Research and Applications ; 25 (2017), 7. - S. 545-552
https://dx.doi.org/10.1002/pip.2832

Degradation and regeneration in mc-Si after different gettering steps

Annika Zuschlag*†, Daniel Skorka† and Giso Hahn

University of Konstanz, Department of Physics, 78457 Konstanz, Germany

ABSTRACT

Light and elevated temperature induced degradation (LeTID) affects significantly the performance of multicrystalline (mc) Si passivated emitter and rear cell (PERC) solar cells, and underlying mechanisms of LeTID are still unknown. In this work LeTID and following regeneration of an industrial mc Si PERC solar cell is compared to differently processed minority charge carrier lifetime samples under illumination (1 sun) and elevated temperature (75 °C). LeTID on cell level reveals the same kinetics compared to lifetime samples. Varying the processing sequence has a significant effect on LeTID of life time samples. Ungettered samples with fired SiN_x:H surface passivation show a very strong LeTID and regeneration effect, with degradation kinetics being similar for all wafer areas irrespective of initial material quality. In contrast, regeneration sets in earlier in good quality areas. Differently gettered samples with lower contamination level than ungettered samples are less sensitive to LeTID, while overall degradation and regeneration behavior is strongly influenced by applied gettering sequences. Al gettered samples show a more pronounced degradation effect than P gettered samples, leading to the as sumption that P gettering is more effective in the reduction of LeTID sensitive defects. If the gettering step is less effective, in lifetime samples after degradation a beginning regeneration effect could be observed. A model is presented, describing LeTID in boron as well as gallium doped mc Si being based on impurities that can be gettered and redistributed during high temperature steps. Using this experimental approach helps to clarify the underlying mechanisms of LeTID and leads to a better understanding of degradation and regeneration mechanisms in mc Si.

KEYWORDS

degradation; regeneration; multicrystalline; silicon; LeTID; gallium

***Correspondence**

Annika Zuschlag, University of Konstanz, Department of Physics, 78457 Konstanz, Germany

E mail: annika.zuschlag@uni konstanz.de

†These authors have contributed equally to this work.

1. INTRODUCTION

Light and elevated temperature induced degradation (LeTID) is a recently discovered effect on multicrystalline (mc) Si passivated emitter and rear cell (PERC) solar cells [1 3]. This effect can cause efficiency losses up to almost 10% rel. under illumination and elevated temperature [3] and cannot be attributed to standard BO complex forma tion or FeB pair dissociation [1]. In mc Si PERC solar cell concepts, a high diffusion length (or high minority charge carrier lifetime, respectively) can be used to further in crease cell efficiency to values >21% [4]. In contrast, for standard full area Al back surface field cells the high bulk material quality does not lead to higher efficiencies be cause of the limiting recombination at the cell's rear side. Therefore, LeTID can be a showstopper when applying PERC technology to mc Si for reaching higher efficiencies.

Also, a regeneration process after degradation has been observed by Kersten *et al.* [3], resembling the behavior known for BO correlated carrier induced degradation and regeneration [5 7], but on a totally different time scale (as already mentioned in [3]). The kinetics of degradation and regeneration is influenced by illumination and temper ature, while the underlying mechanisms causing the degra dation and regeneration of mc Si PERC solar cells are still unknown.

Recent investigations to clarify the parameters influenc ing the degradation and regeneration process are mainly based on solar cell or even on module level. Investigations on lifetime samples are still rare. Kersten *et al.* [3] have demonstrated the degradation of lifetime samples with

different surface passivations, while Krauss *et al.* [8] used spatially resolved minority charge carrier lifetime maps to calculate a so called effective defect lifetime allowing an imaging of effective defects activated upon degradation. Bredemeier *et al.* [9] have recently published a lifetime study on the influence of different firing temperatures on the lifetime degradation and regeneration.

Studying LeTID on solar cell level allows evaluation of the effect directly by current voltage measurements with all effects present (metallization, current distribution in the cell, *etc*.). The advantage of lifetime studies is that a more flexible design of experiment is possible (e.g. regard ing applied process steps/sequences), which can be useful to identify further parameters influencing degradation and regeneration behavior. This work demonstrates minority charge carrier lifetime degradation and regeneration on mc Si wafer level. The different gettering sequences result in different contamination levels and impurity distribu tions. Because of its flexibility, the approach chosen in this contribution based on lifetime samples allows to gain a more detailed fundamental understanding of the underly ing mechanisms of LeTID.

2. EXPERIMENTAL

An industrial mc Si PERC solar cell and several lifetime samples are investigated to compare the degradation and regeneration process on solar cell and lifetime level. The investigation of mc Si PERC solar cells allows one to link and compare the results to previously published results on LeTID, while the studies on differently processed lifetime samples are focused on identification of process steps influencing degradation and regeneration behavior of mc Si material.

The mc Si wafers (1.5 Ωcm boron doped) used for life time samples originate from the same mc Si ingot and the same ingot height as the investigated standard industrial $156 \times 156\ mm^2$ mc Si PERC solar cell, leading to a compa rable material quality of the initial material. Sister wafers ($5 \times 5\ cm^2$) with comparable grain and defect structure were used to compare the influence of different process steps on degradation and regeneration behavior of the life time samples. A scheme of the applied process sequences is given in Figure 1. The wafers were chemically etched to remove saw damage. Sample A was not further proc essed, and only a surface passivation was realized by firing of a plasma enhanced chemical vapor deposition (PECVD) SiN_x:H layer. For samples B, C, and D, different gettering sequences were applied. Sample B was gettered by a $POCl_3$ diffusion (55 Ω/□), while sample C was gettered by screen printing and firing of an Al contact on the backside. P and Al gettering was combined in case of sample D. Additionally, a PECVD SiN_x:H layer was ap plied to all bare wafer surfaces to protect the wafers from contamination during the following firing step. Afterwards, the SiN_x:H layers as well as the Al back surface field and the emitter were removed. The samples were surface passivated again by firing (measured wafer temperature: 730 °C) of a PECVD SiN_x:H layer (same deposition pa rameters as before) leading to an additional hydrogenation of the investigated samples.

For degradation, lifetime samples as well as the solar cell are held at a temperature of approx. 75 °C on a hot plate under illumination with halogen lamps (0.9 ± 0.05 suns for lifetime samples, 1 ± 0.05 sun for the solar cell).

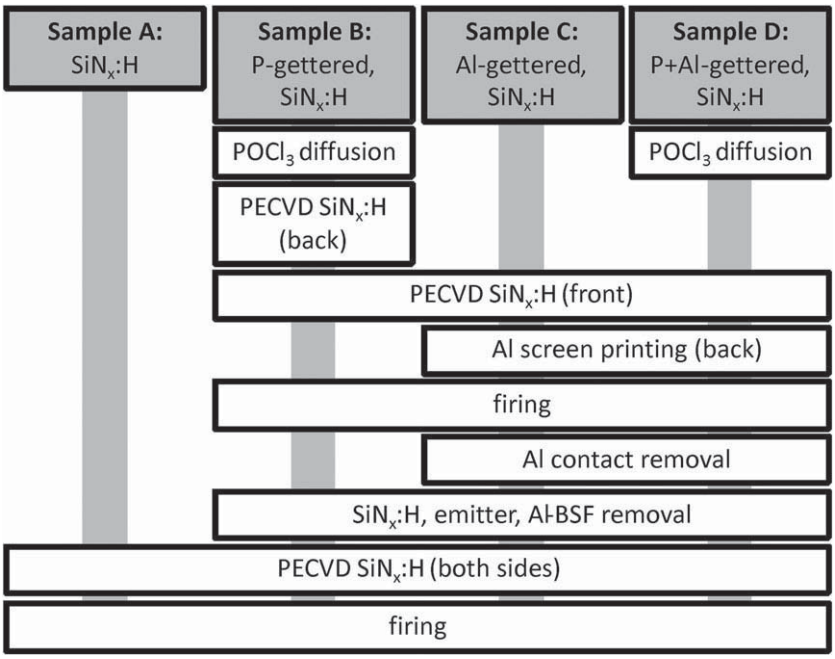

Figure 1. Process sequence of the investigated lifetime samples.

During the degradation and regeneration process, the solar cell is characterized *in situ* by automated open circuit voltage (V_{oc}) measurements. For lifetime samples, effective minority charge carrier lifetime (τ_{eff}) is measured repetitively by the fast and self calibrated time resolved photoluminescence imaging (TR PLI) method [10,11] at room temperature, resulting in a series of spatially resolved lifetime maps for each sample over degradation time. The first τ_{eff} data point of the lifetime samples is measured directly (approx. 2 min) after the last firing step consistent with standard solar cell characterization, which usually takes place directly after firing in industrial production lines.

For a statistically relevant analysis of areas differing in material quality, the TR PLI lifetime maps of each sample over time are aligned and an array of 2500 areas (each $150 \times 150\,\mu m^2$ in size) at fixed positions is distributed over the TR PLI lifetime map of the $5 \times 5\,cm^2$ mc Si samples to get good statistics. Average τ_{eff} values within these areas are extracted over degradation time and further analyzed. This method allows tracking of changes in τ_{eff} of different sample areas under degradation conditions. The advantage of this approach is that the spatially resolved information of τ_{eff} maps over degradation time can be easily displayed. The τ_{eff} data for each $150 \times 150\,\mu m^2$ area on the samples is plotted over time and coded by a rainbow color bar based on the areas' lifetime values at the beginning of the degradation experiment.

3. RESULTS AND DISCUSSION

Continuously measured V_{oc} data of an industrial mc Si PERC solar cell are shown in Figure 2. It is obvious that this PERC solar cell is LeTID sensitive and the V_{oc} data shows a degradation of approx. 12% rel. after 200 h followed by regeneration as also observed previously, for example, in [3]. After 1500 h, the solar cell recovers almost completely. As already discussed in, for example, [1,3] the observed degradation and regeneration cannot be fully explained by BO correlated degradation or FeB pair dissociation processes.

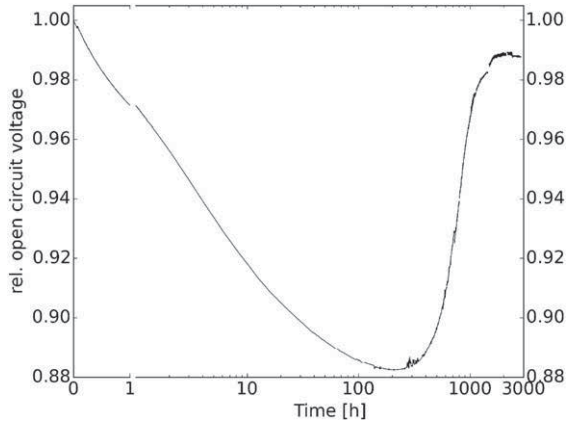

Figure 2. Continuously measured V_{oc} data of an industrial mc Si PERC solar cell showing degradation and regeneration (first 1 h: linear scale, afterwards: log scale).

Figure 3 shows the behavior of harmonic average τ_{eff} for the four differently processed lifetime sister samples A–D. All samples show fast degradation within the first minutes which could be attributed to FeB- and/or BO-based degradation effects. After longer periods, significant differences are measured for samples A, B, C, and D regarding the strength of the degradation, the range of minimum and maximum τ_{eff} in dependence of the degradation state, and the regeneration behavior which can be clearly observed for sample A and also slightly for samples C and D. The ungettered sample A shows the strongest degradation but also the strongest relative regeneration. Applied gettering steps (samples B, C, D) reduce the degradation effect significantly. While samples with Al gettering step (sample C and D) show a lifetime minimum because of degradation, no clear minimum could be observed in case of the only P gettered sample B.

First investigations on a set of gallium doped mc Si lifetime samples with and without P gettering step result in a slower degradation at the beginning of the experiment, most probably because of missing BO- or FeB-induced degradation, strengthening the hypothesis that other impurities are responsible for the so called LeTID effect, as already observed by Ramspeck *et al.* [1] on solar cell level. Also for gallium doped lifetime samples, the degradation in ungettered samples is more pronounced compared to P gettered samples [12]. It is still unclear at this moment whether LeTID can be avoided by replacing B with Ga doping as the concentration of B in the investigated Ga doped samples has not been determined yet.

A comparison to the degradation behavior of the solar cell shows that the maximum degradation level for average τ_{eff} in Figure 3 and the V_{oc} value in case of the solar cell (Figure 2) is reached after approximately the same

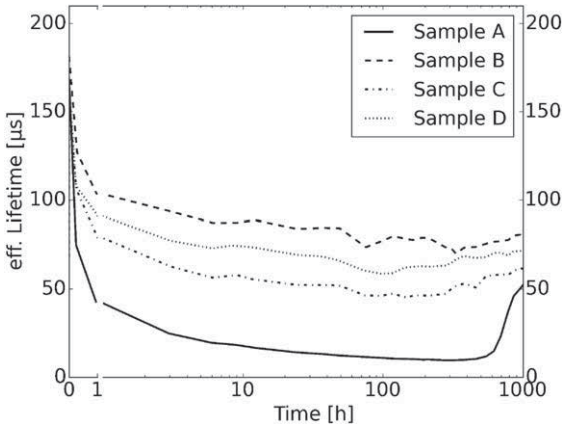

Figure 3. Harmonic average τ_{eff} data for differently processed mc Si wafers. Degradation and regeneration behavior of lifetime samples can be strongly influenced by previously applied gettering sequences (first 1 h: linear scale, afterwards: log scale).

degradation time using (almost) the same illumination level and elevated temperature. This leads to the assumption that the underlying degradation and regeneration effect can be studied either on lifetime or on solar cell level.

The disadvantage of average τ_{eff} analyses is that information on local lifetime distribution measured by spatially resolved TR PLI gets lost. Figure 4 shows exemplarily τ_{eff} maps of sample A at three different states: at the beginning of the degradation, in the degraded state, and during the regeneration process. The whole series of these spatially resolved TR PLI measurements has been aligned and analyzed as described above. Further analyses of the degradation and regeneration behavior will be discussed based on Figure 5. Each single line (guides to the eye connecting single data points) in Figure 5 represents one of the 2500 small $150 \times 150\,\mu m^2$ areas on the lifetime samples.

The applied color code, based on the initial lifetime of each sample at the beginning of the experiment, shows that for all four samples the relative τ_{eff} distribution is maintained during the experiment, which means that independently of the applied process sequence, sample areas with the highest initial τ_{eff} show also the highest τ_{eff} at the maximum degradation level as well as during the regeneration process. This holds true even if the range of lifetime is narrowed down during degradation or is spread again during regeneration.

In case of sample A (not gettered, Figure 5a), a very strong and fast degradation of the whole sample is observed. As already mentioned for harmonic average τ_{eff} data, FeB and/or BO induced degradation could be involved additionally to LeTID in the first few minutes, but the degradation behavior cannot be fully explained based on FeB and/or BO induced dynamics. Especially sample areas of higher initial τ_{eff} suffer from the applied degradation conditions, and relative degradation in these areas is stronger than in sample areas with lower initial τ_{eff}.

The initial lifetime distribution of sample A (approx. 30 350 µs) narrows down to a very small range (approx. 5 30 µs) at maximum degradation level. This strong degradation even in areas of initially high τ_{eff} could be explained by an approximately homogenous formation of defects over the wafer area. The degradation kinetics is very similar in all sample areas, independently of the initial τ_{eff}. After approximately 300 h, a regeneration process sets in, with regeneration in areas with higher initial τ_{eff} (red lines) starting significantly earlier than in areas of lower initial τ_{eff}, indicated by a black dashed line in Figure 5a, and also by the inlay and the differently colored arrows in Figure 5a. The earlier onset of regeneration in areas of initially high τ_{eff} is the reason why in these regions the minimal visible τ_{eff} level is reached earlier compared to areas with lower initial τ_{eff}. But it has to be assumed that initially good τ_{eff} areas show very similar degradation kinetics (time constants) than initially poor τ_{eff} areas. The different starting points for observable regeneration are remarkable, especially regarding the narrow τ_{eff} distribution at around 200 h. The different regeneration behavior leads to the assumption that the regeneration is not only a reversal of the first degradation reaction and that the underlying mechanism is more complex. It is not yet clear whether τ_{eff} recovers completely.

Up to now, it is not yet clear whether the observed degradation within the first hours under illumination originates from bulk defect formation or changes in surface passivation quality. Therefore, an additional sample is prepared exactly like sample A, and the same degradation conditions are applied leading to a comparable degradation behavior as observed for sample A. After approx. 300 h, the SiN_x:H surface passivation layer is etched back and a chemical surface passivation (iodine ethanol, [13]) is applied. The previously measured spatial distribution of low τ_{eff} values after 300 h degradation is thereby confirmed, verifying that the observed strong degradation is a bulk effect and not related to changes in SiN_x:H surface passivation quality. There are hints that SiN_x:H surface passivation quality slightly decreases after several hundred hours under illumination at 75 °C. This might influence the long time regeneration behavior (>1000 h), but cannot explain the observed degradation.

The P gettered sample B (Figure 5b) shows only a slight lifetime reduction within the first minutes under illumination at elevated temperature and is therefore significantly less sensitive to LeTID than sample A. In contrast to the ungettered sample A discussed above, the τ_{eff} range (approx. 40 360 µs) is only slightly narrowed down and stays nearly constant during the experiment. The data shows no clear maximum degradation level and no regeneration, and τ_{eff} stays almost constant in the different

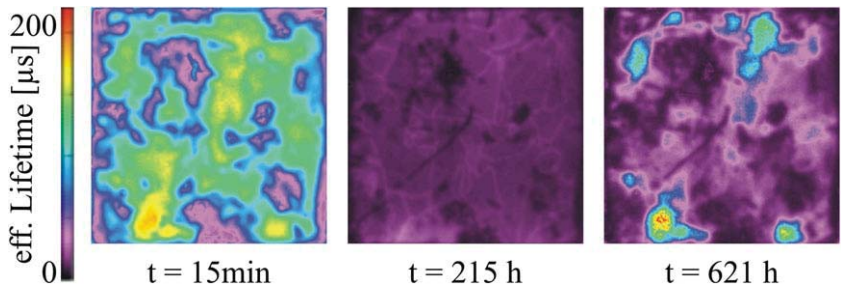

Figure 4. Spatially resolved TR PLI measurements of sample A at the beginning of the applied degradation process, in the degraded state, and during regeneration. [Colour figure can be viewed at wileyonlinelibrary.com]

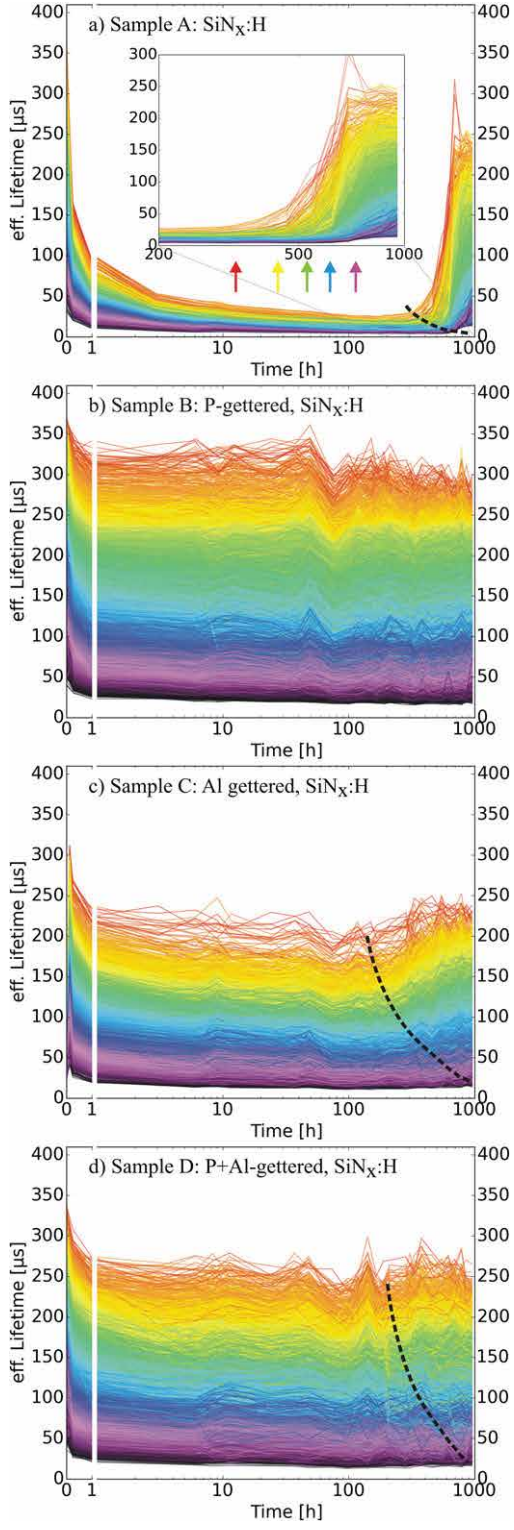

Figure 5. τ_{eff} of differently processed sister wafers (first 1 h: linear scale, afterwards: log scale). Each line in the graph represents an area of 150 × 150 µm^2 in the spatially resolved TR PLI lifetime measurements and is color coded to its value at the beginning of degradation. Black dashed lines indicate beginning regeneration. [Colour figure can be viewed at wileyonlinelibrary.com]

sample areas. Areas of lower initial lifetime after gettering show more relative degradation than areas of higher material quality.

In case of sample B, the repetition of the PECVD SiN_x:H deposition and firing as shown in Figure 1 has been performed to get a similar temperature load compared to the Al gettered samples C and D. If the degradation conditions are applied to a P gettered sample after the first firing of the SiN_x:H passivation layer, comparable results to sample B are observed on an additional wafer set with comparable initial material quality. If the investigated sample area is strongly dominated by extended defect clusters of lower material quality, a more pronounced degradation could be observed also for P gettered samples (not shown). This hints towards a complex interaction of gettering efficiency on local defect structures (as seen, e.g. in [14]) and the effect on degradation behavior.

In contrast to sample B, the Al gettered sister sample C shows a significantly different degradation and regeneration behavior. Overall degradation and regeneration behavior is closer to the ungettered sample A than to the P gettered sample B. As observed for sample A, the Al gettered sample C shows also a maximum degradation level and a narrowing of the τ_{eff} range, but by far not as significant as sample A. The regeneration process again sets in earlier for sample areas with higher initial τ_{eff} as indicated by a black dashed line in Figure 5c.

For sample D, both Al and P gettering were applied. Degradation is stronger than in case of sample B but less pronounced compared to sample C. Also a beginning regeneration can be hinted as indicated by a black dashed line in Figure 5d. Therefore, the degradation and regeneration behavior of sample D is a mix of the observed results of the only P gettered sample B and the only Al gettered sample C.

Because of the expected different contamination level or impurity distribution of the gettered samples B, C, and D compared to sample A, it is assumed that impurities strongly influence the degradation and regeneration behavior. A P gettering step seems to be more efficient to remove degradation sensitive defects than an Al gettering step. After P gettering, each following temperature step leads to a redistribution of (internally or externally) gettered degradation relevant defects. Besides firing steps, the temperature loads during surface passivation processing steps have to be taken into account. In [15], P gettered lifetime samples with different surface passivation treatments (including stack systems like $AlO_x + SiN_x$:H and a thermal SiO_2 covered by SiN_x:H) are compared. It can be demonstrated that for samples with additional temperature load after the P gettering step a more pronounced LeTID and following regeneration occurs. The effect is most pronounced for a thermal SiO_2 step with the highest temperature load, followed by samples with additional AlO_x deposition, while samples with single PECVD SiN_x:H layer show a similar behavior as discussed above for sample B.

It has to be mentioned that the firing conditions (set parameters) are kept constant but lead to a slightly different temperature load of the bulk material during the first firing step for sample B compared to samples C and D because of the screen printed Al back side of samples C and D. The lower wafer temperature of the P gettered sample B compared to the additionally Al gettered sample D during the first firing step may lead to a slightly different and less LeTID sensitive impurity distribution for sample B. As shown in [9], different firing temperatures generally have an influence on degradation behavior.

The earlier onset of regeneration for LeTID in areas of higher τ_{eff} resembles the behavior of regeneration of BO correlated degradation. There it could be shown that a higher excess charge carrier density Δn in the Si bulk leads to a faster regeneration process [6,7]. Interestingly, the onset of LeTID regeneration starts earlier in the best quality areas of sample C (after approx. 200 h) having higher τ_{eff} as compared to the best areas of sample A (after approx. 400 h) as indicated by the dashed line in Figure 5, with sample D lying in between. Note that all samples are sister wafers with comparable extended defect structure and similar surface passivation quality. As higher τ_{eff} leads to higher Δn for constant illumination, this leads to the conclusion that Δn might play a decisive role for LeTID regeneration.

The next step in the analogy between regeneration for LeTID and BO regeneration would be the assumption that hydrogen plays an important role, too. As shown for BO regeneration, the presence of hydrogen in the Si bulk seems to be a prerequisite for the regeneration to occur and its concentration influences the regeneration kinetics [16]. The significantly different time scale could, for example, be explained by the different effective diffusion constant of hydrogen at relatively low temperatures in mc Si compared to monocrystalline Si because of trapping (trap assisted diffusion). But this hypothesis still has to be confirmed in future experiments.

4. MODEL FOR LETID AND CONSEQUENCES

Effective gettering seems to be a key component to minimize the impact of LeTID in mc Si. Under the assumption that degradation in mc Si at longer timescales (>1 h at 75 °C) is triggered by the concentration of a specific impurity (or a mix of impurities) that is more or less homogeneously distributed over the wafer area, a first rough model can be introduced.

In areas of good material quality (low density of extended defects like grain boundaries and/or dislocations) where gettering is very effective, LeTID can be suppressed very effectively in lifetime samples. In contrast, in areas of poorer crystal quality (more extended defects), gettering is less effective as impurities might also be present in the form of precipitates that are harder to getter externally, because they first have to be dissolved and dissolved impurities might be gettered internally again at extended defects. This can be seen qualitatively for sample B (Figure 5b), where good sample areas show less relative degradation than areas of poorer quality, and is also observed in [17] for a different set of samples and different processing sequences.

A consequence of this first model is that high temperature steps after the gettering steps might lead to a redistribution of gettered impurities from their initial gettering sites (e.g. the emitter region, internal gettering sites). Indeed, it could be observed that a thermal oxidation step carried out after a P gettering step “reactivates” LeTID and following regeneration [15].

The model presented here is most probably not yet able to explain LeTID and regeneration behavior in all its facets, but gettering seems to play an important role and should be considered in further experiments to deepen the understanding of LeTID in mc Si.

The regeneration observed for LeTID might be related to the presence of hydrogen in the Si bulk, being more mobile under illumination, maybe because of the change of its charge state [18,19].

Another consequence from the proposed model is that a back to back P diffusion process as normally carried out in industrial cell processing might lead to a stronger LeTID effect because of the less effective gettering.

5. SUMMARY AND OUTLOOK

The influence of different solar cell gettering steps on LeTID and regeneration has been demonstrated using spatially resolved data from TR PLI. It could be shown that the behavior of lifetime samples resembles the behavior of PERC solar cells fabricated from the same mc Si material and can therefore be regarded as relevant for PERC type solar cell processing.

The applied data processing allows the analysis of different sample areas over degradation time in a statistically relevant way and is not limited to selected sample areas or the comparison of only two degradation or regeneration states.

For ungettered samples, it could be shown that degradation kinetics are very similar for all sample areas irrespective of their initial quality, while regeneration sets in first in good quality areas. Gettering drastically reduces LeTID while the strength of degradation and the following regeneration is influenced by the applied gettering sequence. P gettering is more efficient than Al gettering for removing or restructuring LeTID sensitive defects, but gettering efficacy depends also on the underlying crystal defect structure.

It could be shown that LeTID is a bulk degradation effect occurring in boron as well as gallium doped mc Si. Therefore, it cannot be attributed to BO or FeB related defects alone.

The influence of the different gettering sequences on the degradation and regeneration process leads to the

conclusion that the concentration and distribution of (metal) impurities play a major role for LeTID and regen eration. Therefore, the industrial PERC solar cell process ing sequence should be optimized concerning effective gettering and avoidance of redistribution of gettered impu rities during following temperature steps. In addition, a high concentration of hydrogen in the correct binding state might help to speed up the regeneration process (as for BO regeneration [20]), when LeTID cannot be avoided completely.

This long time experiment is still running to further an alyze the regeneration process and the longtime stability of the regenerated state and the surface passivation. Also, ad ditional lifetime samples with further process sequences are under investigation.

ACKNOWLEDGEMENTS

The authors would like to thank Lisa Mahlstaedt and David Sperber for help during sample processing and Axel Herguth for help during sample characterization and fruit ful discussions. Part of this work was funded by the Ger man Federal Ministry of Economic Affairs and Energy and by industrial partners within the research project "SolarLIFE" (0325763B) and within 0325581. The content is the responsibility of the authors.

REFERENCES

1. Ramspeck K, Zimmermann S, Nagel H, Metz A, Gassenbauer Y, Birkmann B, Seidl A. Light induced degradation of rear passivated mc Si solar cells. Pro ceedings 27th EU PVSEC, 2012; 861 865, DOI: 10.4229/27thEUPVSEC2012 2DO.3.4
2. Fertig F, Krauss K, Rein S. Light induced degradation of PECVD aluminium oxide passivated silicon solar cells. *Physica Status Solidi (RRL)* 2014; **9**(1): 41 46. DOI:10.1002/pssr.201409424.
3. Kersten F, Engelhart P, Ploigt HC, Stekolnikov A, Lindner T, Stenzel F, Bartzsch M, Szpeth A, Petter K, Heitmann J, Müller J. Degradation of multicrystalline silicon solar cells and modules after il lumination at elevated temperature. *Solar Energy Ma terials & Solar Cells* 2015; **124**: 83 86. DOI:10.1016/j.solmat.2015.06.015.
4. Green MA, Emery K, Hishikawa Y, Warta W, Dunlop ED. Solar cell efficiency tables (version 47). *Progress in Photovoltaics: Research and Applications* 2016; **24**(1): 3 11. DOI:10.1002/pip.2728.
5. Herguth A, Schubert G, Kaes M, Hahn G. A new ap proach to prevent the negative impact of the metastable defect in boron doped Cz silicon solar cells. Proceed ings 4th WCPEC, 2006; 940 943.
6. Herguth A, Schubert G, Kaes M, Hahn G. Investiga tions on the long time behavior of the metastable boron oxygen complex in crystalline silicon. *Progress in Photovoltaics: Research and Applications* 2008; **16**: 135 140. DOI:10.1002/pip.779.
7. Herguth A, Hahn G. Kinetics of the boron oxygen re lated defect in theory and experiment. *Journal of Ap plied Physics* 2010; **108**: 114509 1 7. DOI:10.1063/ 1.3517155.
8. Krauss K, Fertig F, Menzel D, Rein S. Light induced degradation of silicon solar cells with aluminium oxide passivated rear side. *Energy Procedia* 2015; **77**: 599 606. DOI:10.1016/j.egypro.2015.07.086.
9. Bredemeier D, Walter D, Herlufsen S, Schmidt J. Life time degradation and regeneration in multicrystalline silicon under illumination at elevated temperature. *AIP Advances* 2016; **6**: 035119 1 8. DOI:10.1063/ 1.4944839.
10. Kiliani D, Micard G, Steuer B, Raabe B, Herguth A, Hahn G. Minority charge carrier lifetime mapping of crystalline silicon wafers by time resolved photoluminescence imaging. *Journal of Applied Phys ics* 2011; **110**: 054508 1 7. DOI:10.1063/1.3630031.
11. Kiliani D, Herguth A, Micard G, Ebser J, Hahn G. Time resolved photoluminescence imaging with elec tronic shuttering using an image intensifier unit. *Solar Energy Materials & Solar Cells* 2012; **106**: 55 59. DOI:10.1016/j.solmat.2012.05.042.
12. Zuschlag A, Skorka D, Hahn G. Comparison of degra dation and regeneration kinetics in differently doped mc Si materials. To be published.
13. Pollock K, Junge J, Hahn G. Detailed investigation of surface passivation methods for lifetime measurements on silicon wafers. *IEEE Journal of Photovoltaics* 2012; **2**(1): 1 6. DOI:10.1109/jphotov.2011.2174337.
14. Gindner S, Karzel P, Herzog B, Hahn G. Efficacy of phosphorus gettering and hydrogenation in multicrystalline silicon. *IEEE Journal of Photovoltaics* 2014; **4**(4): 1063 1070. DOI:10.1109/ JPHOTOV.2014.2322276.
15. Zuschlag A, Skorka D, Hahn G. Degradation and re generation analysis in mc Si. Proceedings 43rd IEEE PVSC, 2016, in press.
16. Wilking S, Herguth A, Hahn G. Influence of hydrogen on the regeneration of boron oxygen related defects in crystalline silicon. *Journal of Applied Physics* 2013; **113**: 194503 1 6. DOI:10.1063/1.4804310.
17. Skorka D, Zuschlag A, Hahn G. Spatially resolved degradation and regeneration kinetics in mc Si. Pro ceedings 32nd EU PVSEC, 2016; 643 646, DOI: 10.4229/EUPVSEC20162016 2AV.1.26.
18. Hamer P, Hallam B, Wenham S, Abbott M. Manipula tion of hydrogen charge states for passivation of p type

wafers in photovoltaics. *IEEE Journal of Photovoltaics* 2014; **4**(5): 1252 1260. DOI:10.1109/JPHOTOV.2014.2339494.

19. Sun C, Rougieux FE, Macdonald D. A unified approach to modelling the charge state of monatomic hydrogen and other defects in crystalline silicon. *Journal of Applied Physics* 2015; **117**: 045702. DOI:10.1063/1.4906465.
20. Wilking S, Herguth A, Hahn G. Influence of bound hydrogen states on BO regeneration kinetics and consequences for high speed regeneration processes. *Solar Energy Materials & Solar Cells* 2014; **131**: 2 8. DOI:10.1016/j.solmat.2014.06.027.